Thermoreversible gelation in aqueous dispersions of colloidal particles bearing grafted poly(ethylene oxide) chains

Jennifer S. Shay

Department of Chemical Engineering, North Carolina State University, Raleigh, North Carolina 27695-7905

Srinivasa R. Raghavan

Department of Chemical Engineering, University of Delaware, Newark, Delaware 19716

Saad A. Khan[a)]

Department of Chemical Engineering, North Carolina State University, Raleigh, North Carolina 27695-7905

(Received 8 September 2000; final revision received 29 March 2001)

Synopsis

Colloidal interactions between particles in a dispersion can be tuned by grafting polymeric chains onto the surface of the particles. The affinity between the polymeric chains and the continuous-phase liquid controls the strength of these interactions. In our system the polymer–liquid affinity is strongly influenced by temperature, and as a result, dramatic changes occur in the dispersion microstructure on heating. The system is an aqueous dispersion of polystyrene (PS) particles bearing grafted poly(ethylene oxide) (PEO) chains of low molecular weight ($\sim$ 2000). At room temperature, water is a good solvent for PEO chains, and the dispersion is a stable, low-viscosity sol. As temperature is increased, water becomes a progressively worse solvent for PEO. Beyond a temperature T_c there is a sharp transition in microstructure from a stable sol to a volume-filling gel. The sol–gel transition is reversible and the transition temperature T_c can be pinpointed using tan δ versus temperature plots. Remarkably, T_c is more than 100 °C lower than the θ temperature for PEO (2000) in water, i.e., the gelation occurs under *significantly better-than-*θ conditions. T_c is independent of particle concentration, but is strongly influenced by the graft density of PEO chains on the particles. The higher the graft density, the higher the T_c for gelation; conversely, at very low graft density, the samples are gels even at room temperature. Above T_c, the elastic modulus (G') of the gels reveals a power law dependence with particle volume fraction (ϕ), i.e., $G' \propto \phi^n$. The power law exponent n is independent of the PEO graft density, implying that the various gels have a similar microstructure. We suggest that gelation is the result of a weak secondary minimum in the interparticle potential that can develop in the case of short stabilizing moieties and moderate solvent conditions.
[DOI: 10.1122/1.1378030]

[a)]Author to whom correspondence should be addressed; electronic mail: khan@eos.ncsu.edu; Tele: 919-515-4519; Fax: 919-515-3465

I. INTRODUCTION

Control of colloidal dispersion stability is of great importance for a variety of applications including food products, oil recovery, and coatings. Colloidal particles inherently tend to flocculate due to attractive van der Waals forces, and one way to counteract this is by grafting polymeric chains to the surface of the particles. The polymeric chains provide a steric barrier to flocculation, thus giving rise to a stabilized dispersion (sol) [Russel *et al.* (1989)]. An important variable, however, is the solvent quality of the dispersion medium for the stabilizing chains. Stability is ensured only if the medium is a good solvent for the chains; on the contrary, if solvency is sufficiently diminished, the particles may flocculate. A link between particle flocculation and the θ point for the polymer–solvent pair is now firmly established for stabilizing chains of high molecular weight ($> 10^4$) and at high surface coverage [Napper (1977)].

Our focus is on a disperse system in which the affinity between solvent and stabilizing chains is strongly influenced by temperature. The system is an aqueous dispersion of polystyrene (PS) particles to which we have chemically grafted low molecular-weight poly(ethylene oxide) (PEO) chains, using a novel urethane linkage to bind the PEO chains to the particle surface [Shay (1999)]. As is well known, increasing the temperature decreases the solvent quality of water for PEO chains, with a closed-loop miscibility gap evidenced in the PEO–water phase diagram [Saeki *et al.* (1976)]. We study the effects of temperature on our dispersions using rheology and dynamic light scattering (DLS). Our principal finding is that a *sol–gel transition* occurs in concentrated systems when heated beyond a critical temperature. Thus, increasing the temperature transforms the sample from a stable, low-viscosity sol to a colloidal gel with a yield stress. The system of PS particles with grafted PEO chains is a popular one in the literature, and the rheology in the stable regime has been studied in detail [Prestidge and Tadros (1988); Ploehn and Goodwin (1990); Liang *et al.* (1992)]. Our focus is on the temperature-induced transition to instability, which despite its unusual nature, has attracted limited attention [Liang *et al.* (1993)]. In particular, we use rheology to confirm the presence and conditions of the sol–gel transition, apply the Winter–Chambon criterion [Winter and Chambon (1986)] to identify the gel point, and probe the origin of this phenomenon in terms of the underlying colloidal forces.

II. EXPERIMENT

A. Synthesis and preparation of latex dispersions

The PS particles with grafted PEO were synthesized by dispersion polymerization. Methyl-endcapped PEO chains (MW $\sim$ 2000), functionalized with a urethane endgroup, were incorporated into the reaction mixture to allow *in situ* grafting of the chains to the surfaces of the developing PS latex particles. Further details of the synthesis procedure can be found elsewhere [Shay (1999); Shay *et al.* (2000a, 2000b)]. The particles were in the 250–300 nm range in diameter and were relatively monodisperse. Particles with three different PEO graft densities were synthesized by varying the weight ratio of PEO relative to styrene in the synthesis mixture. The L6, L12, and L24 latexes correspond to 6%, 12%, and 24% respectively, of PEO to styrene by weight. Transmission electron microscopy and proton nuclear magnetic resonance confirm the presence of grafted PEO chains on the surface of the particles, with the density of grafted chains increasing linearly with the above weight ratio. Following synthesis, the latex dispersions were cleaned exhaustively through a series of centrifugations using distilled de-ionized water. Dispersions were subsequently diluted with de-ionized water to the appropriate weight fraction. Volume fractions were calculated using the true density of PS.

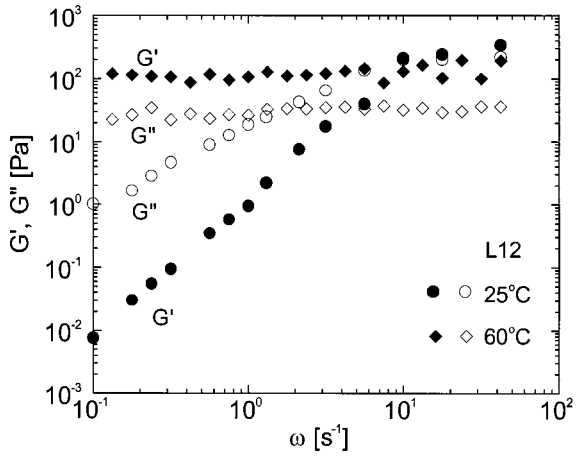

FIG. 1. Elastic (G') and viscous (G'') moduli as functions of frequency (ω) for the L12 latex dispersion (intermediate PEO graft density) at $T = 25\,°C$ and 60 °C. The volume fraction ϕ of the disperse phase is 0.1.

B. Rheology

Rheological measurements were performed on a Rheometrics Dynamic Stress Rheometer using a couette fixture. The cell was heated by a reservoir of water circulating from a PolySciences high temperature bath. A solvent trap was used to prevent evaporation from the sample. The system was equilibrated for at least 30 min at each temperature prior to experimentation. Both steady and dynamic rheological experiments were conducted at each temperature.

C. Dynamic light scattering (DLS)

DLS was performed using an argon-ion laser of wavelength 514.5 nm (Coherent Innova) and a BI-9000 correlator (Brookhaven Instruments). The measurements were performed in the angular range of 60°–120° (no angle dependence was generally found). Sample temperature was controlled by a circulating water bath. The autocorrelation function was analyzed by the method of cumulants to yield a diffusion coefficient, which was used in conjunction with the Stokes–Einstein relationship to obtain a hydrodynamic radius (assuming sphericity).

III. RESULTS

Dynamic frequency spectra depicting the elastic (G') and viscous (G'') moduli as functions of frequency are shown in Fig. 1 for a representative dispersion of the L12 latex (intermediate graft density), at a volume fraction $\phi = 0.1$. Data are shown for temperatures of 25 and 60 °C. Dramatic changes in the rheology and microstructure of our dispersions are observed between the two temperatures studied. At 25 °C, the dispersion behaves as a low-viscosity fluid, as evidenced by the dominance of the viscous component G'' over the elastic component G' and also the characteristic frequency dependence of the moduli ($G' \sim \omega^2, G'' \sim \omega$). At 60 °C, on the other hand, the sample responds in a predominantly elastic fashion, with G' exceeding G'' over the entire frequency range and with both the moduli being independent of frequency. This indicates that the dispersion has been transformed from a nonflocculated sol into a colloidal gel having a sample-spanning particulate network structure.

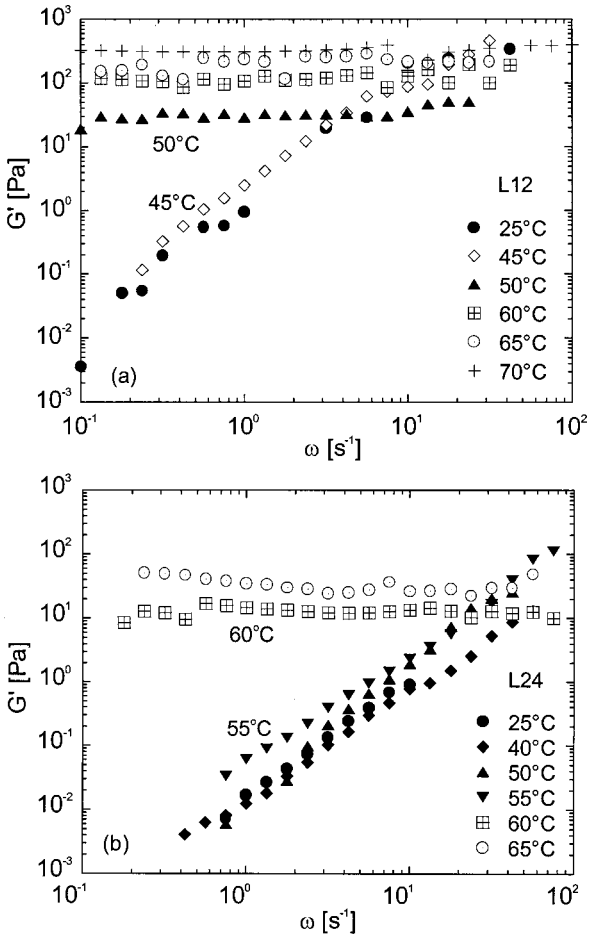

FIG. 2. Elastic modulus (G') as a function of frequency (ω) for dispersions at $\phi = 0.1$ of (a) the L12 latex with moderate PEO graft density and (b) the L24 latex with a high PEO graft density. Data are shown for a range of temperatures between 25 and 65 °C.

To confirm the singular location of the sol–gel transition, we systematically monitored the dynamic rheological behavior over a series of temperatures between 25 and 70 °C. This is presented in Fig. 2(a) for the L12 latex (moderate graft density) and in Fig. 2(b) for the L24 latex (high graft density) (both dispersions are at $\phi = 0.1$). We show only the elastic modulus G' since it sufficiently illustrates the evolving microstructure. At low temperatures, each sample is a stable, nonflocculated sol and displays liquid-like rheology ($G' \sim \omega^2$). As temperature is increased, each sample shows a sharp sol–gel transition within a narrow temperature range, as indicated by the shift from a frequency-dependent to a frequency-independent G' profile. Past the transition, the magnitude of G' (i.e., the gel modulus) continues to rise with temperature.

In the spirit of the Winter–Chambon gel point criterion, we attempted to identify the precise sol–gel transition temperature from the above data [Winter and Chambon (1986); Coviello and Burchard (1992)]. For this, the loss tangent $\tan\delta (= G''/G')$ is plotted as a function of temperature for various frequencies (Fig. 3). As per the above criterion, the point where $\tan\delta$ is independent of frequency is the gel point. We find the constant frequency lines for both samples to have common points of intersection, implying that the

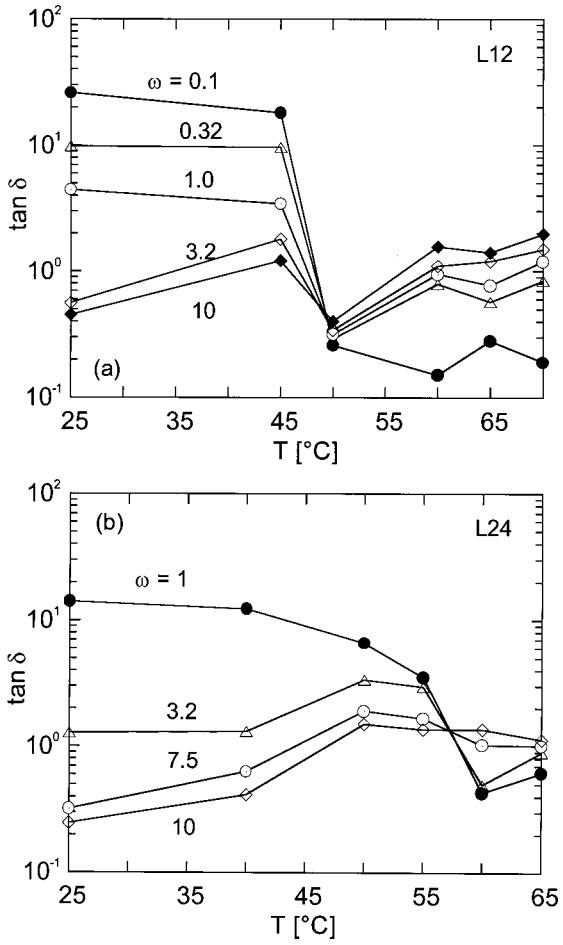

FIG. 3. Loss tangent (tan $\delta = G''/G'$) as a function of temperature (T) plotted from the data in Fig. 2. The point of intersection is the temperature of the sol–gel transition. For the L12 dispersion (a), the point of intersection places the sol–gel transition at 49 °C, and the point of intersection for the L24 dispersion (b) is at 57 °C.

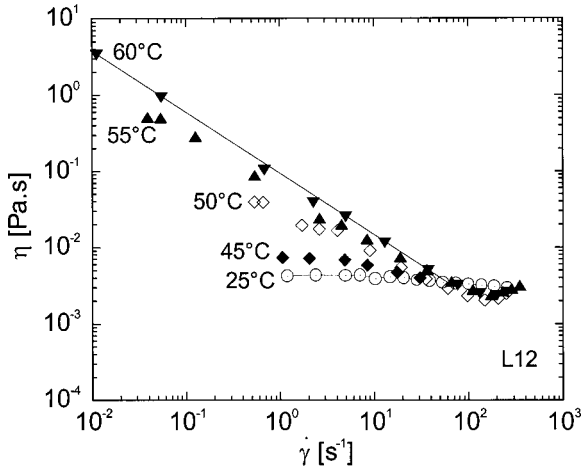

FIG. 4. Steady shear viscosity (η) as a function of shear rate ($\dot{\gamma}$) for the L12 dispersion ($\phi = 0.1$) at temperatures ranging from 25 to 60 °C.

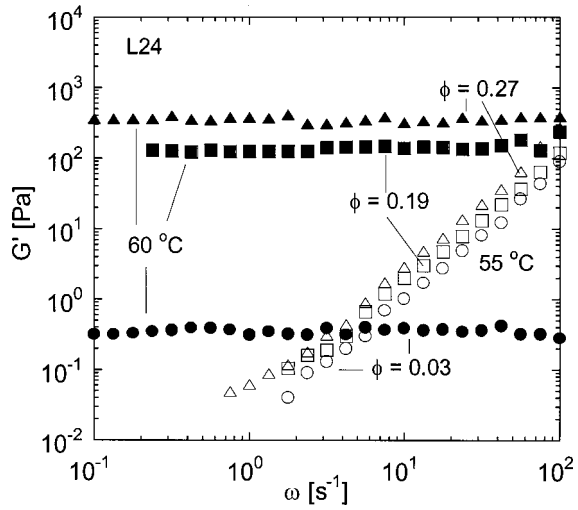

FIG. 5. Elastic modulus (G') as a function of frequency (ω) for dispersions of the L24 latex at various particle volume fractions (ϕ). Data is shown at 55 and 60 °C in each case (below and above the sol–gel transition temperature). Volume fraction of the dispersions are given by: circles (0.03), square (0.19), and triangles (0.27).

systems follow the Winter–Chambon criterion and possess a self-similar structure at the gel point. For the L12 sample [Fig. 3(a)], tan δ values merge into a single point at $T_c \approx 49\,°\mathrm{C}$ which is then the sol–gel transition temperature. For the L24 sample, the sol–gel transition occurs at a higher temperature ($\approx 57\,°\mathrm{C}$) [Fig. 3(b)]. Thus, increasing the graft density increases the transition temperature as well.

Striking changes are also observed under steady-shear rheometry around the sol–gel transition temperature (Fig. 4). At low temperatures, the L12 sample is a low-viscosity Newtonian fluid, consistent with the dynamic rheological data presented above. Around the sol–gel transition temperature ($T_c \approx 49\,°\mathrm{C}$), there is a rise in the low-shear viscosity along with the appearance of shear thinning at higher shear rates. At even higher temperatures, the sample develops a yield stress (as indicated by a slope of -1 in the log–log plot of viscosity versus shear rate). These changes indicate the formation of flocs in the sample around T_c and their eventual development into a colloidal network.

Varying the particle concentration has little effect on T_c, as found by comparing dispersions of L24 at different volume fractions ϕ between 0.03 and 0.27 (Fig. 5). At a temperature of 55 °C ($T < T_c$) the samples show practically identical values of the frequency-dependent G'. In each case, the sol–gel transition is complete at 60 °C, consistent with the T_c value of 57 °C obtained from the tan δ plot for the $\phi = 0.1$ sample [Fig. 3(b)]. The magnitude of the gel modulus G', measured at a constant temperature above T_c, increases with the particle concentration ϕ in the dispersion.

At much lower concentrations ($\phi \sim 10^{-3}$), we resorted to DLS to probe changes in the dispersion structure. Analysis of the data were kept at its simplest. The data are reported in terms of an average hydrodynamic diameter d_{app} of spherical particles (assuming that any flocs formed are also spherical) as a function of temperature for the L12 and L24 samples (Fig. 6). Consistent with the rheological experiments, DLS reveals a sharp rise in the scattered intensity around T_c for both systems, which translates into an increase in the apparent particle diameter as shown by the plots. This confirms the formation of particulate flocs for $T > T_c$.

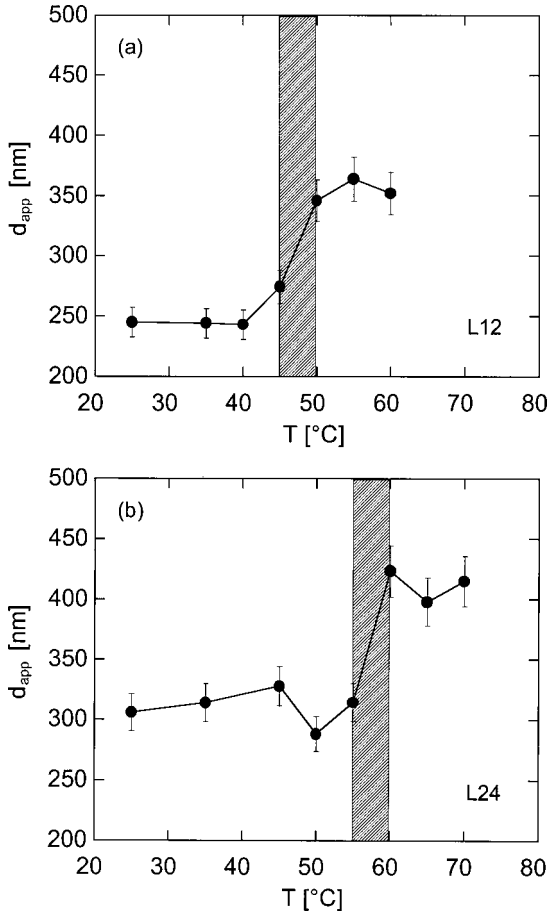

FIG. 6. Average hydrodynamic diameter (d_{app}) as a function of temperature for dilute dispersions ($\phi \sim 10^{-3}$) of (a) the L12 latex and (b) the L24 latex, as measured by dynamic light scattering (DLS). The shaded regions represent the location of the sol–gel transition as seen in the rheological profiles of the materials.

The rise in scattered intensity can also be detected visually in the case of dilute samples, which appear clear and colorless at ambient temperature. On heating to T_c, the sample turns cloudy (cloud point), and further heating reveals visible flocs. The sample reverts to a clear and homogeneous state on cooling, indicating that the transition is reversible. Concentrated dispersions are opaque with a milky white appearance, and do not lend themselves to visual detection. However, a sample below T_c flows readily on inverting a test tube, whereas above T_c it flows very slowly or not at all, indicating its gel-like nature. The flowable state is regained on cooling, suggesting that the phenomenon under study has a thermodynamic origin.

Quantitative measurements of thermoreversibility were also undertaken using both rheology and light scattering. Figure 7(a) shows d_{app} for the L12 latex as temperature is increased from 25 °C to the gelation temperature (*viz.* 50 °C), and then reduced back to 25 °C. The apparent particle diameter d_{app} increases significantly on heating and then decreases to its original value upon cooling. Reversibility is also apparent in the rheological data, as shown for a representative L24 sample in Fig. 7(b). A sol–gel transition occurs on heating from 55 to 60 °C and the sol state is regained on cooling back to 55 °C.

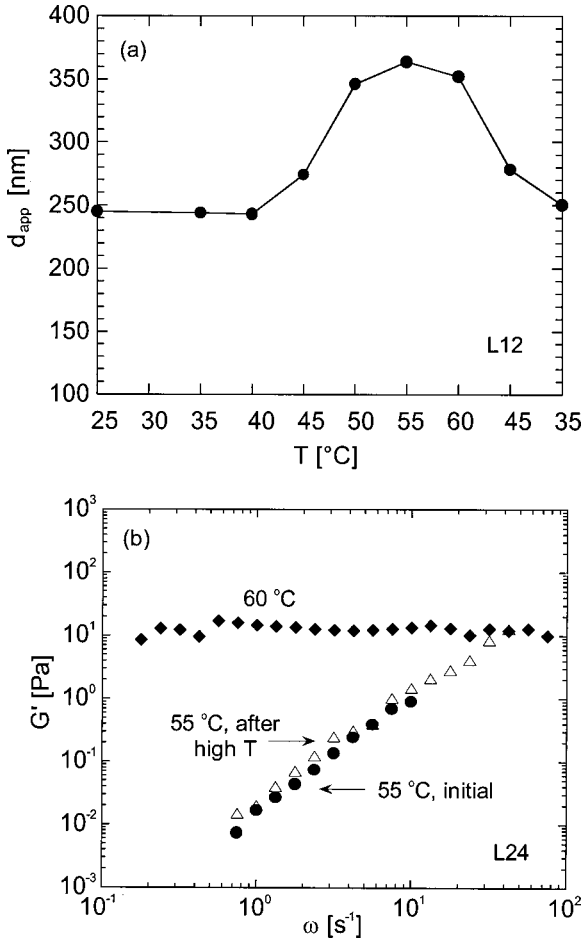

FIG. 7. (a) Average apparent particle diameter (d_{app}), as measured by DLS, of a dilute dispersion ($\phi \sim 10^{-3}$) of the L12 latex as temperature is increased from 25 to 50 °C, and then reduced back to 25 °C. (b) Elastic modulus (G') vs frequency (ω) for the L24 system ($\phi = 0.1$) showing the sol–gel transition between 55 and 60 °C as temperature is increased, and then a gel–sol transition in the same temperature range as temperature is decreased.

Experiments were also performed with the L6 latex particles, which have a low graft density of PEO chains. These particles form colloidal gels at room temperature and for volume fractions as low as $\phi = 0.03$ [Fig. 8(a)]. Even at low volume fractions ($\phi \sim 10^{-5}$), dynamic light scattering provides evidence for flocculation (data not shown) [Shay (1999)]. Thus, the L6 particles readily flocculate, whereas L12 and L24 particles can form stable, nonflocculated sols at low temperatures. Heating the L6 gels ($\phi = 0.1$) causes the gel modulus G' to steadily increase [Fig. 8(b)], and G' at 60 °C is an order-of-magnitude higher than at 25 °C. Thus, the rheology of L6 samples is steadily enhanced on heating, but there are no abrupt changes as observed for the L12 and L24 systems.

Further microstructural information can be deduced by comparing the gel modulus G' at a constant temperature for the L6, L12, and L24 systems as a function of particle volume fraction ϕ (Fig. 9). The data were obtained at 60 °C, which is above the sol–gel transition in all cases; thus, each system is in the ''gel'' regime where G' is independent

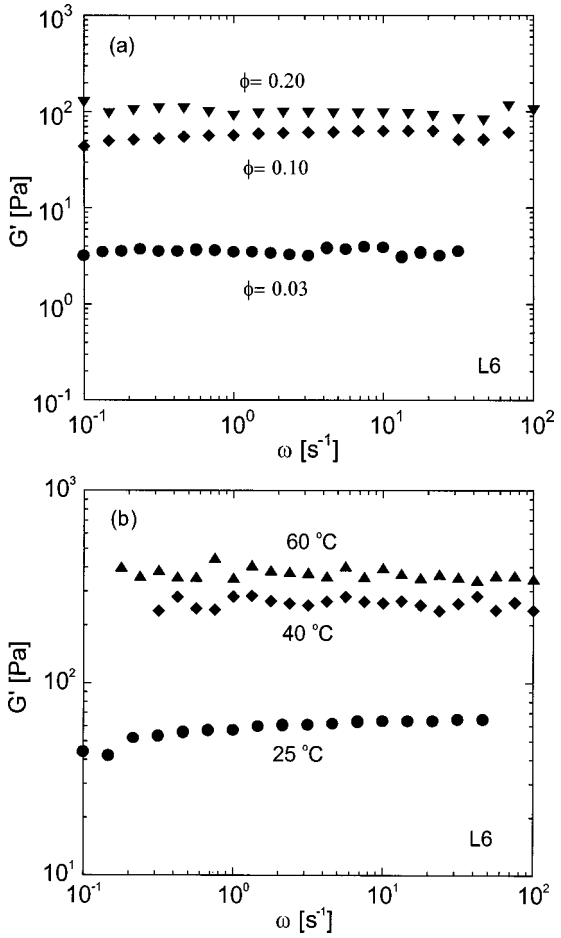

FIG. 8. (a) Elastic modulus (G') as a function of frequency (ω) for dispersions of the L6 latex (low graft density) at $T = 25\,°C$. Data are shown for various particle volume fractions ranging from $\phi = 0.03$ to 0.20. (b) Elastic modulus (G') vs frequency (ω) at various temperatures for a dispersion of the L6 latex (low graft density). The particle volume fraction $\phi = 0.1$.

of frequency. In each case, G' shows a power-law behavior ($G' \propto \phi^n$), with the G' value at a fixed ϕ decreasing in the order L6 $>$ L12 $>$ L24. The power-law index n is ~ 3.5 for all three systems, suggesting that the gel microstructure is independent of graft density (Khan and Zoeller, 1993). Note that 3.5 is the predicted exponent for diffusion-limited cluster–cluster aggregation [Buscall *et al.* (1988)]. It should, however, be pointed out that detailed analysis of the fractal nature of the gel moduli and mechanism of gel formation at different temperatures is not within the scope of this work.

IV. DISCUSSION

To interpret the data, we first recognize that the sol–gel transition in our system occurs under *better-than-*θ conditions. In fact, water is not a θ solvent for PEO of molecular-weight 2000 over the temperature range studied [Napper (1970); Saeki *et al.* (1976)]. The phase diagram for PEO (2000) in water (LCST) does show a closed-loop miscibility gap, but the lower consolute solution temperature ($\approx$ the θ temperature) occurs only at

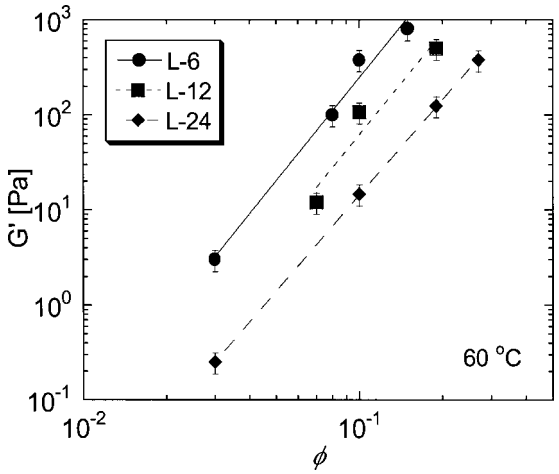

FIG. 9. Elastic modulus (G') as a function of particle volume fraction (ϕ) for dispersions of the L6, L12, and L24 latices, which differ only in their PEO graft densities. The data were taken at 60 °C (in the flocculated regime of all three dispersions) where G' is independent of frequency.

176 °C [Saeki *et al.* (1976)]. The sol–gel transition in our systems, on the other hand, is complete by about 60 °C—i.e., more than 100 °C removed from θ conditions.

The flocculation observed in our system is thus *not* the incipient flocculation observed at the θ point in sterically stabilized dispersions [Napper (1977)]. In the latter case, flocculation is dictated by the osmotic free energy V_{osm} upon mixing of polymeric chains from two adjacent particles, which varies as $V_{\text{osm}} \sim (1/2-\chi)$, where χ is the Flory–Huggins parameter for the polymer–solvent pair. Past the θ point, χ exceeds 1/2; thus, V_{osm} changes sign from repulsive to attractive, and the particles flocculate. Flocculation at the θ point has been demonstrated previously for PEO-stabilized dispersions. For example, dispersions of PEO-stabilized particles in 0.39 M $MgSO_4$ flocculate exactly at their θ temperature, provided the PEO molecular weight is sufficiently high (at least 6000) [Napper (1970)].

When the molecular weight of the stabilizing moieties is low, however, flocculation can occur under better-than-θ conditions [Garvey (1977); Cowell and Vincent (1982); Liang *et al.* (1993)]. For example, PS particles with grafted PEO (2000) flocculated in 0.3 M Na_2SO_4 on heating to $\sim$ 35 °C, and at even lower temperatures in more concentrated salt solutions [Liang *et al.* (1993)]. No comparisons with θ conditions were made by the authors, but these systems clearly flocculate under better-than-θ conditions (e.g., θ = 67 °C for PEO in 0.3 M Na_2SO_4 [Boucher and Hines (1976)]). Note that in these studies, a divalent electrolyte was used, which worsens the solvent quality of water for PEO chains, and so the θ temperatures are relatively low. Our dispersions, on the other hand, are electrolyte-free and hence have higher θ temperatures.

The question then is what causes flocculation in our systems at temperatures far removed from θ conditions? Evidently, the underlying cause is the deteriorating solvent quality of water for PEO (2000) chains with increasing temperature. This deterioration occurs progressively as thermal motion breaks down the hydrogen bonds between PEO and water (thus, the ethylene oxide units become increasingly hydrophobic) [Kjellander and Florin (1981)]. Indeed, measurements of water activities in aqueous, electrolyte-free PEO solutions show that temperature significantly affects water activity even for short polymer chains and low temperatures (30–60 °C) [Eliassi *et al.* (1999)].

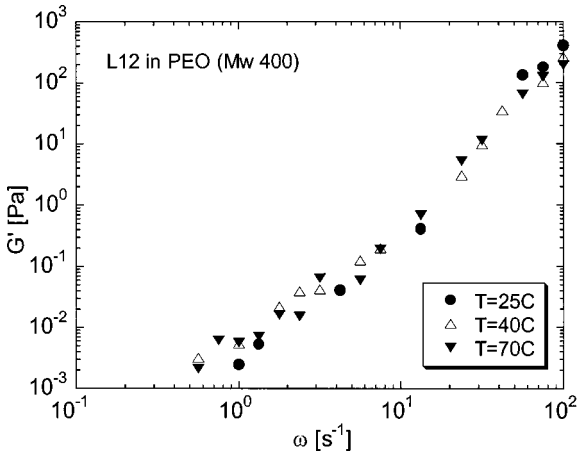

FIG. 10. Elastic modulus (G') vs frequency (ω) for dispersions of the L12 latex in a PEO melt (MW $\sim$ 400). The particle volume fraction ϕ is 0.1 and data are shown for temperatures between 25 and 70 °C.

Another way to demonstrate the importance of solvent quality in directing flocculation is to replace water by other solvents, an intriguing possibility being a PEO melt. In the latter case, the grafted PEO (2000) chains on the particles will be in a medium consisting of chemically identical moieties, and the enthalpic interaction between polymer and solvent will hence be nearly zero [Smitham and Napper (1976)]. To examine this scenario, we prepared dispersions of L12 and L24 particles in a PEO melt (of molecular weight $\sim$ 400). Dispersions over a range of particle concentrations were studied as a

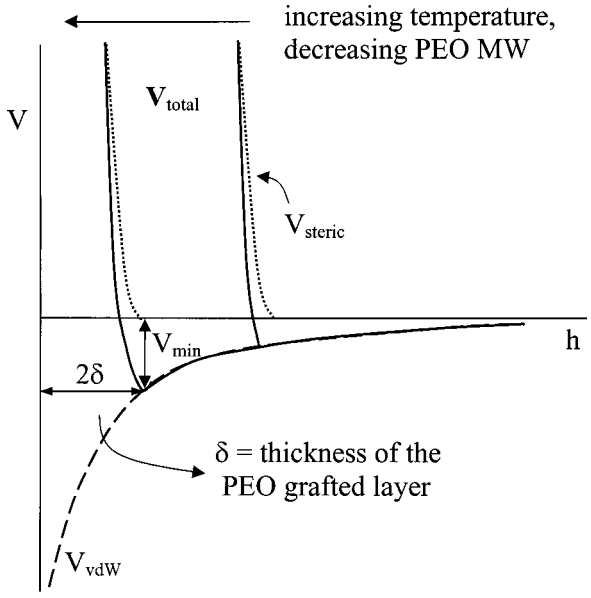

FIG. 11. Schematic representation of the interparticle potential V as a function of the separation distance h between the particles. The total potential V_{total} is depicted as solid lines, while the contributions from steric interactions (V_{steric}) and van der Waals interactions (V_{vdW}) are shown as dashed and dotted lines, respectively. The scenarios for two different temperatures or molecular weights of the stabilizing moieties are depicted.

function of temperature. Rheology showed that the dispersions were stable sols over the entire temperature range. Figure 10 is a typical plot from dynamic rheology for L12 particles at $\theta = 0.1$ in PEO (400), and it reveals a liquid-like response ($G' \sim \omega^2$) at all temperatures. Thus, there are no microstructural changes with temperature in PEO (400), in contrast to the sol–gel transitions in water.

The temperature-dependent interaction between PEO and water is thus the crucial factor dictating flocculation. We now attempt to understand these phenomena in terms of the pair potential between the colloidal particles. The reversible nature of the sol–gel transition points to a weak attractive minimum in the potential (e.g., a secondary minimum). Such secondary minima can indeed arise in sterically stabilized systems if the stabilizing moieties are of low molecular weight [Garvey (1977)].

The situation is sketched schematically in Fig. 11. Assuming that the electric double-layer repulsion can be neglected, there are two contributions to the total interparticle potential $V_{\text{total}}(h)$: from the attractive van der Waals interaction between the core particles (V_{vdW}) and from the steric interaction between the grafted chains (V_{steric}). In turn, V_{steric} can be broken down into osmotic (V_{osm}) and elastic (V_{elastic}) contributions, among which the latter is always repulsive, while the former is repulsive only in a good solvent for the chains (i.e., $\chi < 1/2$). Note that the steric interaction sets in only at a distance of separation closer than 2δ, where δ is the thickness of the layer of grafted chains. For short (i.e., low molecular-weight) grafted chains, δ will be small and the particles will have to approach to a very short distance for the steric repulsion to become effective. A secondary minimum of magnitude V_{min} can then arise. Longer (i.e., higher molecular-weight) chains give a larger δ and thereby a smaller V_{min}. For sufficiently long chains, there will be no secondary minimum and the potential will be solely repulsive.

The molecular weight of our PEO stabilizers being only 2000, it is conceivable that a secondary minimum could develop in the colloidal pair potential between our particles. Flocculation into such a shallow potential well will be reversible, with the lifetime of a particle–particle encounter depending on the depth of V_{min}. Appreciable flocculation will be detected only when this timescale is long enough or particle collisions to be sustained. A V_{min} that is small at low temperatures and becomes significant on heating to $\sim T_c$ could thus explain the observed sol–gel transition in our systems. We must then correlate the increase in well depth V_{min} with the deterioration in PEO solvency on heating. There are three factors which may play a role in this regard [Garvey (1977); Russel *et al.* (1989)]:

(a) *Magnitude of the steric repulsion*: As solvency is decreased, χ increases and hence the magnitude of the osmotic contribution to V_{steric} decreases. Since V_{steric} is the repulsive part of V_{total}, a decrease in the repulsions means a deeper attractive well V_{min}.

(b) *Range of the steric repulsion*: The thickness of the stabilizing layer δ can decrease with decreasing solvency. The grafted chains will prefer to be in an extended conformation in a good solvent, but will shrink towards the particle surface as solvency decreases. As is clear from Fig. 11, a smaller δ implies a larger V_{min}.

(c) *Bridging interactions*: A bridging attraction between PEO chains on adjacent particles may develop on decreasing the solvency and make an additional contribution to the magnitude of V_{min}.

We can thus see how for the case of low molecular-weight stabilizers, V_{min} can be significant even when the system is far from θ conditions. Flocculation will be appreciable only beyond a critical well depth $V_{\text{min}}^{\text{crit}}$, corresponding to a sufficiently long time-

scale for sustaining particle–particle encounters. This critical depth is evidently reached at the sol–gel transition temperature T_c. Under these conditions, the particles attract and so flocculation (gelation) occurs. At temperatures higher than T_c, the attractive well is expected to deepen, implying even stronger interparticle attractions. Correspondingly, the gel modulus G', which is roughly proportional to the second derivative of the potential versus distance curve, should increase [Russel *et al.* (1989); Raghavan *et al.* (2000)]. Indeed, this is what we observe (Fig. 2). (If the system is further heated to the θ point, the V_{osm} contribution to V_{steric} will become attractive, implying a much deeper V_{min} and possibly leading to irreversible coagulation.)

Among the three contributions to V_{min} listed above, the bridging interaction is the least understood, but it is potentially significant. The calculations of Bjorling (1992) show that bridging attractions can set in between surfaces with grafted PEO chains of low molecular weights such as those here. Bridging is expected to be enhanced when the interaction between PEO and water becomes weak. In that case, the hydrophobic particle surface may develop a higher affinity for the polymer chains than for the water molecules. Bridging occurs when this increased affinity of the particle surface is accommodated by chains from neighboring particles. In other words, bridging corresponds to water disliking both the hydrophobic surfaces as well as the chains, and forcing the chains onto the surfaces. The surface coverage of grafted PEO chains is an important factor in this regard—bridging is significant at low coverages, whereas at high coverages a negligible number of bridges are formed [Bjorling (1992)].

Based on the foregoing arguments, we can also discuss the effect of varying the PEO graft density in our system. We had found that decreasing the graft density lowered the sol–gel transition temperature T_c (Fig. 3), and at very low PEO coverages, gels were formed at all temperatures (Fig. 8). The results imply that at an equivalent temperature, the attractive well depth V_{min} is an inverse function of the graft density—i.e., the lower the graft density, the higher the V_{min}. Such an effect can be rationalized in several different ways. First, lowering the graft density may imply a lower osmotic repulsion, since the volume fraction of polymer chains in the surface layer factors into the magnitude of V_{osm} [Napper (1977)]. A second issue could be the conformation of the PEO chains at low and high coverages [Cosgrove *et al.* (1987)]. At low coverage, the chains would be in rather flat configurations in order to expel as much water as possible from the hydrophobic surface. Alternately, at high coverage, the chains would tend to adopt a more extended conformation normal to the surface as they are restricted in lateral extension parallel to the surface. This would serve to increase the layer thickness δ, and thus reduce V_{min} (Fig. 11). Lastly, the tendency for bridging is expected to be greater at low coverages [Bjorling (1992)], which would again serve to increase V_{min}.

Our results are thus qualitatively consistent with the nature of the interparticle colloidal forces. Clearly, the low molecular weight of our stabilizing chains is implicated as the underlying reason for the flocculation under better-than-θ conditions. This interpretation is consistent with previous studies where the particles in dispersion bear short grafted chains [e.g., Cowell and Vincent (1982); Bergstrom and Sjostrom (1999)]. The reversible flocculation into a shallow potential well (secondary minimum) may thus be viewed as a generic characteristic in such sterically stabilized systems, just as with the analogous flocculation seen in electrostatically stabilized systems.

V. CONCLUSIONS

Aqueous dispersions of PS particles with grafted low molecular-weight PEO chains show a reversible sol–gel transition with increasing temperature. The transition tempera-

ture T_c increases as the graft density of PEO chains increases. This phenomenon occurs under better-than-θ conditions, and can be attributed to a weak attractive minimum in the potential energy of particle interaction. Such a potential minimum $V_{\min}$ is expected to develop when the stabilizing chains are of low molecular weight. Increasing the temperature worsens the solvent quality of water for PEO, thus increasing the depth of $V_{\min}$. A key factor in this regard may be the bridging attraction, i.e., the tendency for PEO-covered particles to form interparticle bridges under conditions of reduced solvency. Ultimately, at T_c, the attractive potential becomes strong enough to sustain interparticle collisions, thus causing macroscopic gelation. Changing the continuous medium from water to a PEO melt eliminates this effect, thus implicating the temperature dependence of the PEO–water interaction as an essential requirement.

ACKNOWLEDGMENTS

The authors wish to acknowledge the U.S. Environmental Protection Agency and a National Science Foundation fellowship (J.S.S.) for funding this work. The authors also thank Sharon Wells (University of North Carolina) for her assistance with the dynamic light scattering measurements.

References

Bergstrom, L. and E. Sjostrom, ''Temperature-induced gelation of concentrated ceramic suspensions: Rheological properties,'' J. Eur. Ceram. Soc. **19**, 2117–2123 (1999).

Bjorling, M., ''Interaction between surfaces with attached poly(ethylene oxide) chains,'' Macromolecules **25**, 3956–3970 (1992).

Boucher, E. A. and P. M. Hines, ''Effects of inorganic salts on the properties of aqueous poly(ethylene oxide) solutions,'' J. Polym. Sci., Part A: Gen. Pap. **14**, 2241–2251 (1976).

Buscall, R., P. D. A. Mills, J. W. Goodwin, and D. W. Lawson, ''Scaling behavior of the rheology of aggregate networks formed from colloidal particles,'' J. Chem. Soc., Faraday Trans. 1 **84**, 4249–4260 (1988).

Cosgrove, T., T. Heath, B. van Lent, F. Leermakers, and J. Scheutjens, ''Configuration of terminally attached chains at the solid-solvent interface: Self-consistent field theory and a Monte Carlo model,'' Macromolecules **20**, 1692–1696 (1987).

Coviello, T. and W. Burchard, ''Criteria for the point of gelation in reversibly Gelling systems according to dynamic light scattering and oscillatory rheology,'' Macromolecules **25**, 1011–1012 (1992).

Cowell, C. and B. Vincent, ''Temperature-particle concentration phase diagrams for dispersions of weakly interacting particles,'' J. Colloid Interface Sci. **87**, 518–526 (1982).

Eliassi, A., H. Modarress, and G. A. Mansoori, ''Measurement of activity of water in aqueous poly(ethylene glycol) solutions (effect of excess volume on the Flory–Huggins χ-parameter),'' J. Chem. Eng. Data **44**, 52–55 (1999).

Garvey, M. J., ''Flocculation of sterically stabilized dispersions under better-than-theta conditions,'' J. Colloid Interface Sci. **61**, 194–196 (1977).

Khan, S. A. and N. J. Zoeller, ''Dynamic rheological behavior of flocculated fumed silica suspensions,'' J. Rheol. **37**, 1225–1235 (1993).

Kjellander, R. and E. Florin, ''Water structure and changes in thermal stability of the system poly(ethylene oxide)-water,'' J. Chem. Soc., Faraday Trans. 1 **77**, 2053–2055 (1981).

Liang, W., Th. F. Tadros, and P. F. Luckham, ''Rheological studies on concentrated polystyrene latex sterically stabilized by poly(ethylene oxide) chains,'' J. Colloid Interface Sci. **153**, 131–139 (1992).

Liang, W., Th. F. Tadros, and P. F. Luckham, ''Influence of addition of electrolyte and/or increase of temperature on the viscoelastic properties of concentrated sterically stabilized polystyrene latex dispersions,'' Langmuir **9**, 2077–2083 (1993).

Napper, D. H., ''Flocculation studies of sterically stabilized dispersions,'' J. Colloid Interface Sci. **32**, 106–114 (1970).

Napper, D. H., ''Steric stabilization,'' J. Colloid Interface Sci. **58**, 390–407 (1977).

Ploehn, H. J. and J. W. Goodwin, ''Rheology of aqueous suspensions of polystyrene latex stabilized by grafted poly(ethylene oxide) chains,'' Faraday Discuss. Chem. Soc. **90**, 77–90 (1990).

Prestidge, C. and Th. F. Tadros, ''Viscoelastic properties of aqueous concentrated polystyrene latex dispersions containing grafted poly(ethylene oxide) chains,'' J. Colloid Interface Sci. **124**, 660–665 (1988).

Raghavan, S. R., J. Hou, G. L. Baker, and S. A. Khan, ''Colloidal interactions between particles with tethered non-polar chains dispersed in polar media: Direct correlation between dynamic rheology and interaction parameters,'' Langmuir **16**, 1066–1077 (2000).

Russel, W. B., D. A. Saville, and W. R. Schowalter, *Colloidal Dispersions* (Cambridge University Press, Cambridge, 1989).

Saeki, S., N. Kuwahara, M. Nakata, and M. Kaneko, ''Upper and lower critical solution temperatures in poly(ethylene glycol) solutions,'' Polymer **17**, 685–689 (1976).

Shay J. S., ''Aqueous colloidal dispersions with grafted poly(ethylene oxide) chains: Synthesis, microstructure, and rheology,'' Ph.D. thesis, North Carolina State University, Raleigh, NC, 1999.

Shay, J. S., R. J. English, R. J. Spontak, C. M. Balik, and S. A. Khan, ''Dispersion polymerization of polystyrene latex stabilized with novel grafted poly(ethylene glycol) macromers in *n*-propanol/water,'' Macromolecules **33**, 6664–6671 (2000a).

Shay, J. S., R. J. English, and S. A. Khan, ''Rheological behavior of a polymerically stabilized latex for use in water-borne coatings,'' Polym. Eng. Sci. **40**, 1469–1479 (2000b).

Smitham, J. B. and D. H. Napper, ''Elastic steric stabilization in polymer melts,'' J. Colloid Interface Sci. **54**, 467–470 (1976).

Winter, H. H. and F. Chambon, ''Analysis of linear viscoelasticity of a cross-linking polymer at the gel point,'' J. Rheol. **30**, 367–382 (1986).